Protein Organization and Pleomorphicity.

Author's Details: [(1)]**Dr. Abdullah Sethar,**D.V.M., M. Sc (Honors) from Pakistan and Ph.D from England, UK.Deputy Project Director,Sindh Agricultural Growth Project (Livestock Component) World Bank Assisted, Government of Sindh, [(2)]**Dr. Benjamin W. Neuman**-School of Biological-University of Reading-UK

Abstract: *The result of density transects analysis of the ends (0^0 and 180^0) vs sides (90^0 and 270^0) of elliptical TCRV are shown in figure 6.7. While the density of the inner and outer membrane peaks remained constant, there was less electron density present in the expected positions of GP, Z and NP on the flat "sides" (90^0 and 270^0) of elliptical TCRV particles. The shape of each peak was similar, but no broadening was observed. This was interpreted to indicate that less protein was present at the expected position for each of the three viral structural proteins, GP, Z and NP. It was further revealed understand the role of protein organization in virion morphology, images of TCRV was manually grouped according to the apparent organization of the Z and NP components. In order to do this, all elliptical TCRV particles were selected and manually rotated to match one of the nine categories shown in Figure 6.5. The number of images in each section therefore reflects the prevalence of each type of organization in the population of elliptical TCRV. As shown in Figure 6.5, the most common organization found displayed well organized Z and NP around the termini of the longest diameter, i.e., at highly curved "ends" of each particle. In contrast, Z and NP organization often appeared to be disrupted at the termini of the shortest diameter, i.e., on the less curved "sides" of each particle. The presence of GP appeared to correlate with protein organization, with GP being present only on regions where organized Z and NP were visible inside the virion. Several of the particles appeared to lack GP on the flat or inwardly curving "sides" of the particle*
Key Words: *Protein, Organization, and Pleomorphicity*

Introduction.

The purpose of this analysis was to measure how much Z and NP is positioned near the edge of the virion. It was yet unknown so we come up with this method to select different sides as briefed to do the transect analysis.

In order to understand protein organization and pleomorphicity images of well-organized and poorly organized arenavirus have been shown and radial density averages have been taken. Radial density transects were taken at 8 points spaced evenly around each particle.

6.1.1 Principles of electron diffraction and electron density.

The diagram below is intended to help describe how the electron beam will be affected as it passes through the different types of atoms that make up the phospholipid envelope and protein constituents of the virion. Basically, the larger the number of electrons, and the greater the number of occupied electron shells, the more apparent contrast will be produced when an electron beam passes through the sample (figure 6.1). For example, the phosphorous atoms found in the headgroup of the phospholipid molecules of the membrane will have a greater apparent electron density compared to proteins, which consist predominantly of the smaller atoms carbon, hydrogen, nitrogen and oxygen [187].

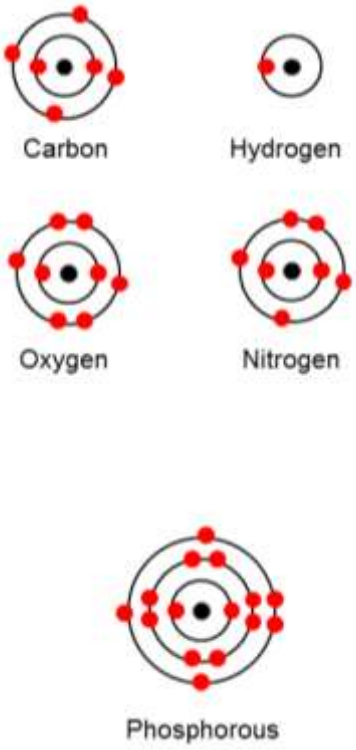

Figure 6:1. This figure shows the amount of electrons in outer and inner layer of viruses.

6.2 Process of radial density:

In order to understand the process of the radial density, what and how it was done is illustrated below. In this process, the image brightness is taken as a surrogate for the relative electron density. Although absolute comparisons are problematic, relative comparisons, for example between matched section of the same virion, are within the scope of this technique. The relationship between structure and apparent electron density is presented in schematic form in figure 6.2.

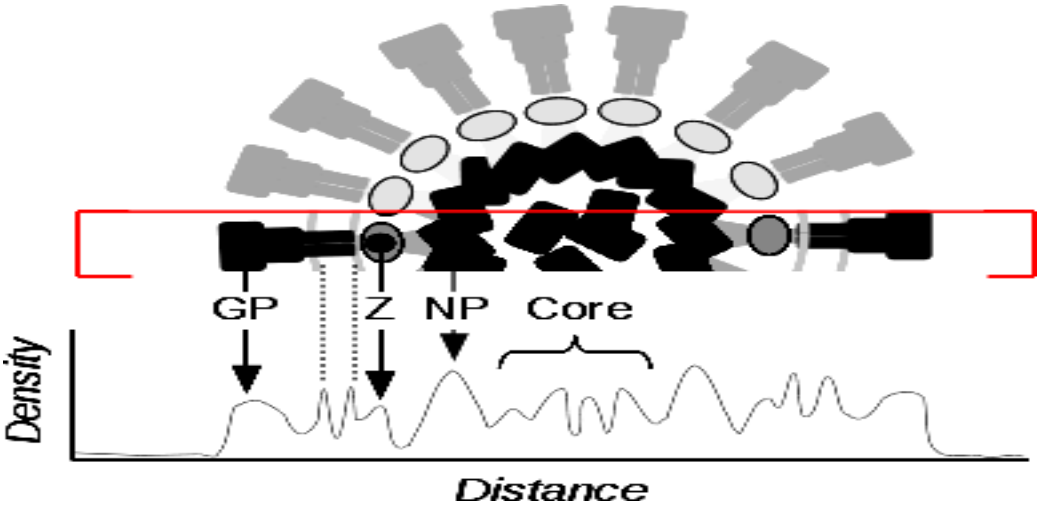

Figure 6.2. The process for measuring relative organization and density of each protein in the viral complex.

In this way eight triplicate samples were taken from around the elongated virions.

One end of the virion, centered on the longest available diameter was initially marked as being at 0^0. Further samples were recorded at ~45^0 intervals such that 0^0 and 180^0 derived from the termini of the maximum diameter and 90^0 and 270^0 from

the termini of the shortest diameter, with one additional sample taken in between each of these. Figure 6.3 shows a virion with one positions of each of the 24 (8×3) samples indicated by a rectangle.

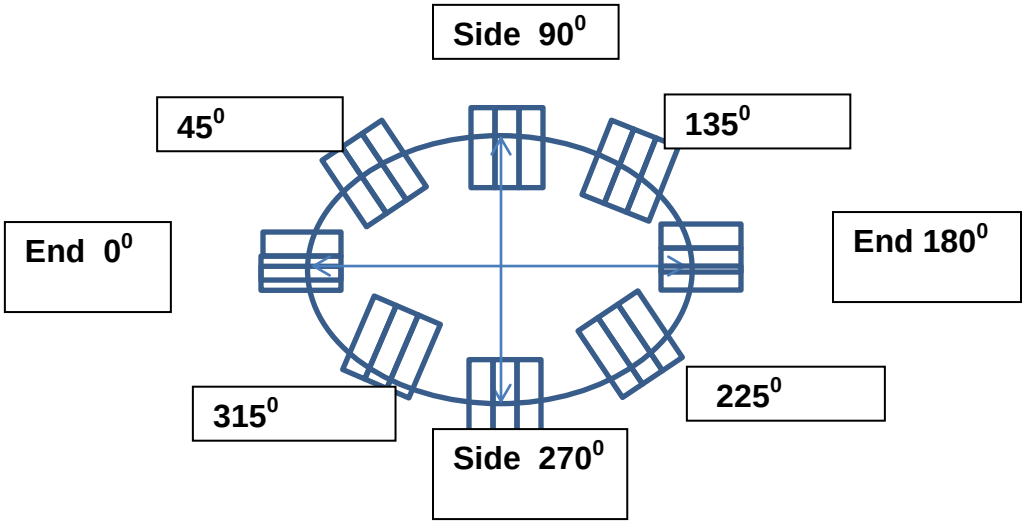

Figure 6:3. Elliptical virion in the position of eight triplicate density transects indicated by rectangles.

6.3 Images of arena viruses:

In order to understand the context of the density transect analysis, images of well-organized and poorly organized elliptical and round viruses are shown below (See figure 6.4).

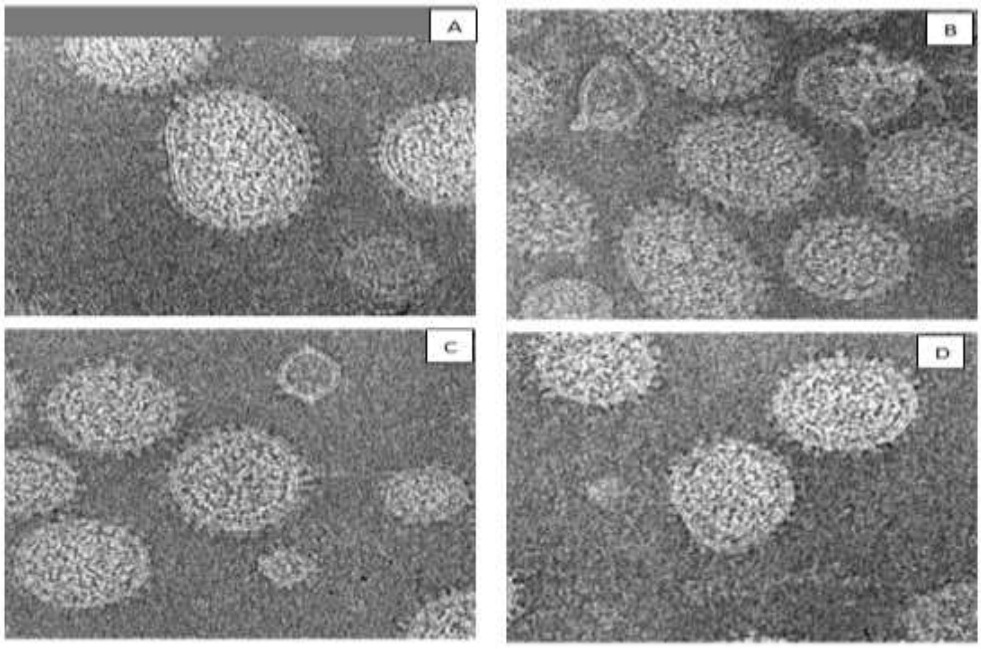

Figure 6.4. (A-B) Showing well organized Z and NP at the curved ends of elliptical particles (C-D) Uniformly good organization of round particle (C) well organized round particles (D) Good organization of round particles.

In order to understand the role of protein organization in virion morphology, images of TCRV were manually grouped according to the apparent organization of the Z and NP components. In order to do this, all elliptical TCRV particles were

selected and manually rotated to match one of the nine categories shown in Figure 6.5. The number of images in each section therefore reflects the prevalence of each type of organization in the population of elliptical TCRV. As shown in Figure 6.5, the most common organization found displayed well organized Z and NP around the termini of the longest diameter, i.e., at highly curved "ends" of each particle. In contrast, Z and NP organization often appeared to be disrupted at the termini of the shortest diameter, i.e., on the less curved "sides" of each particle. The presence of GP appeared to correlate with protein organization, with GP being present only on regions where organized Z and NP were visible inside the virion. Several of the particles appeared to lack GP on the flat or inwardly curving "sides" of the particle. Taken together, this suggests that well-organized protein complexes are usually associated with regions of the membrane where the local curvature approaches that of a sphere of approximately 100 nm diameter.

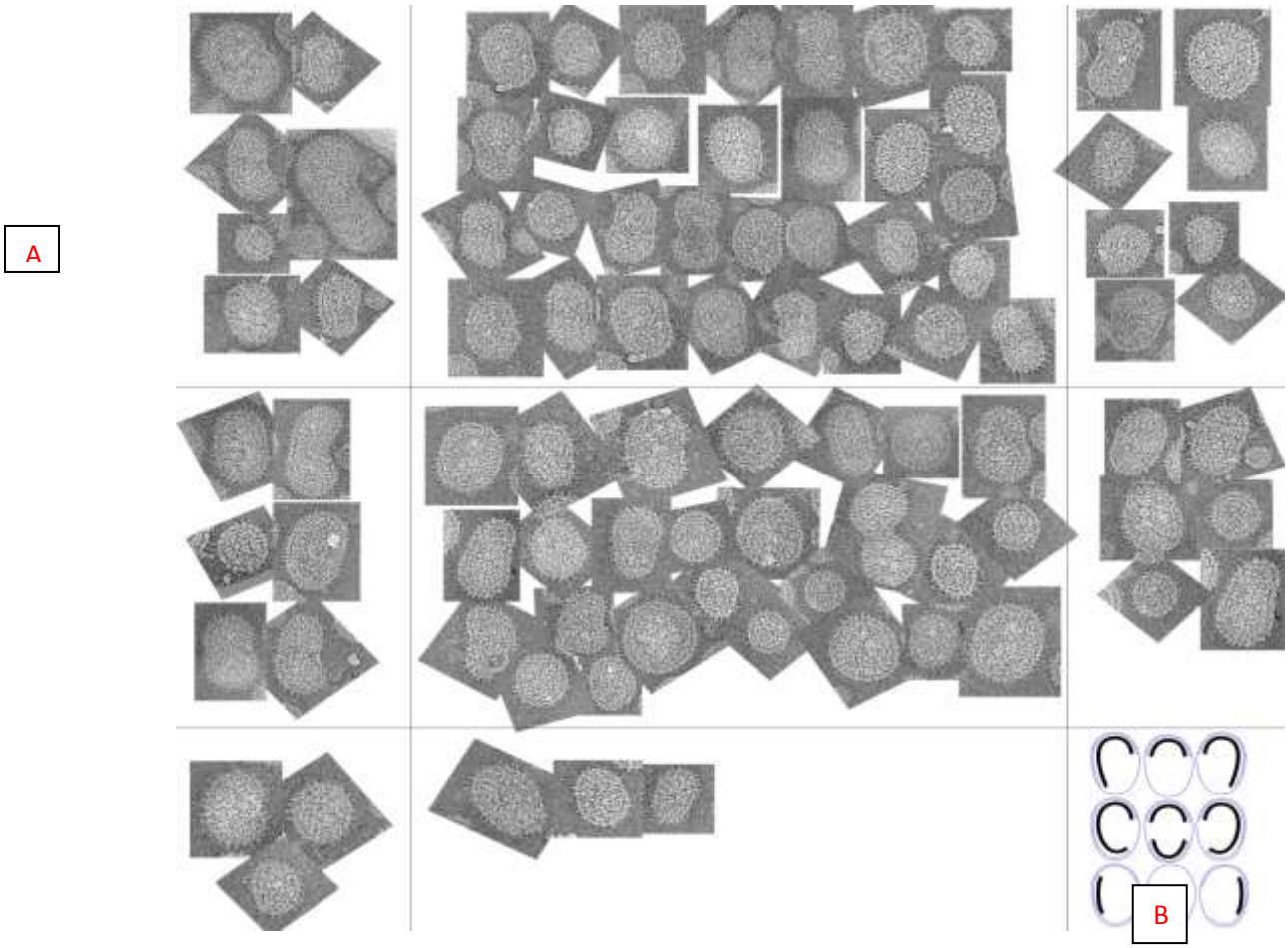

Figure 6.5 (A) TCRV particles grouped by internal organization. Particles are organized according to the key at lower right, which indicates good organization with a thick inner line.

6.4 Radial density average:

In order to understand the radial density non overlapping membrane regions were collected along the entire edge of each viral particle to minimize the distortion caused by small variations in curvature. These images were converted to electron density transects, then aligned and averaged. Radial density values were extracted from these averaged images using SPIDER.

6.5 Transect analysis of TCRV

Figure 6.6 illustrates how density transects were compared. If the area under the curve is the same but the curve is wider then it would be interpreted the amount of protein is same but poorly organized. If the area under the curve is less but the curve is not wider this would be interpreted to mean that there is less protein, but the organization is the still same. A third possibility is that if the area under the curve is less and the curve is wider this would be interpreted to indicate that there is less protein and more disorder.

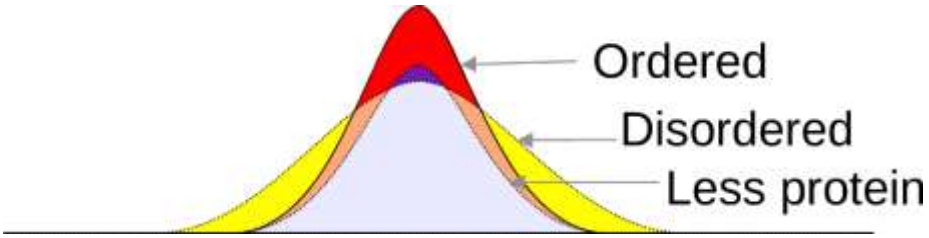

Figure 6:6. This picture shows the protein thickness and density.

6.6 Radial Density average of TCRV:

The results of density transects analysis of the ends (0^0 and 180^0) vs sides (90^0 and 270^0) of elliptical TCRV are shown in figure 6.7. While the density of the inner and outer membrane peaks remained constant, there was less electron density present in the expected positions of GP, Z and NP on the flat "sides" (90^0 and 270^0) of elliptical TCRV particles. The shape of each peak was similar, but no broadening was observed. This was interpreted to indicate that less protein was present at the expected position for each of the three viral structural proteins, GP, Z and NP.

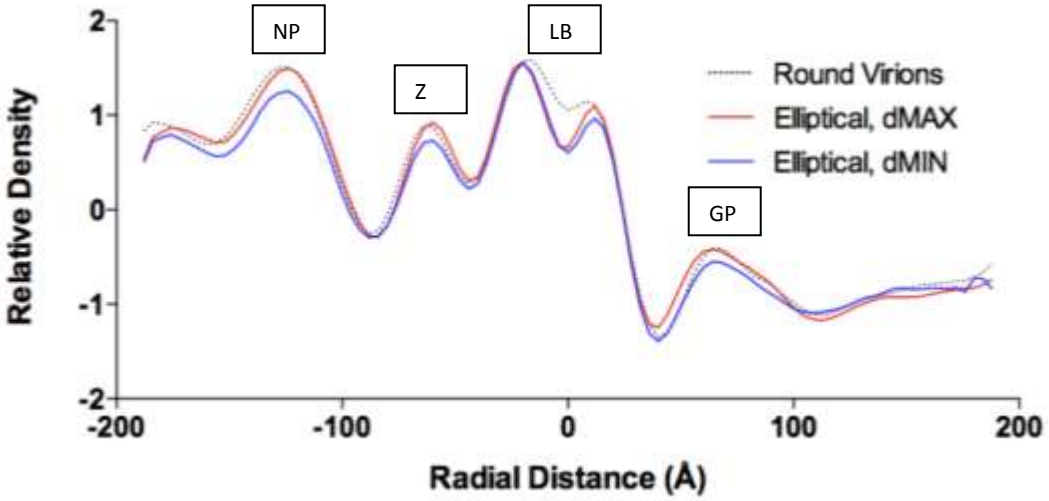

Figure 6.7. Radial Density averages of TCRV. It shows round particle in dotted line and elliptical viruses are shown in red and blue color which were taken from two corners diameter maximum and diameter minimum.

6.7 Density of Arena virus:

In order to understand the density of viruses of all sizes, all TCRV virions, round (n=94) and elliptical (n=119) in total 213 viruses, grouped by size, were selected. Averages for groups of 12 similar-sized virions +/- SEM (dotted lines) were calculated. It was concluded that there is no significant relationship between virion size and apparent density of NP, Z and GP (see figure 6:8). This also demonstrated that different sized particles, which naturally have different local curvatures, give constant density results, meaning that parts of a virion that differ only in curvature as at the ends and sides of elliptical virions, should not differ unless there is a difference in local protein density or architecture.

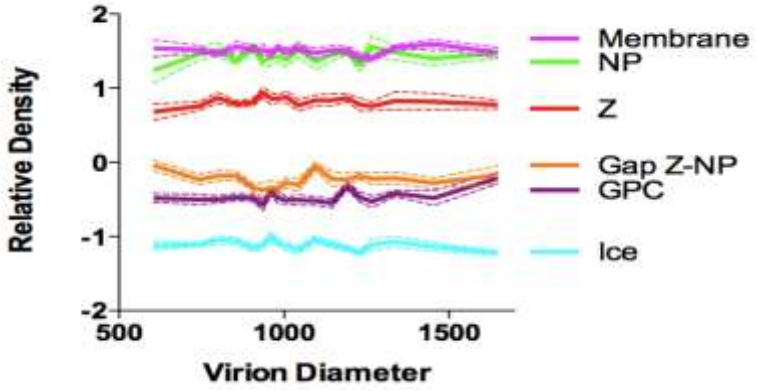

Figure 6:8. The density versus size of arenaviruses. Averages for groups of 12 similar-sized virions +/- standard error of mean (SEM) (dotted lines)

6.8 Comparison of elliptical, intermediate and round particles:

In order to understand the difference between each of separate protein of TCRV, virions were separated into groups of equal size containing data from the most elliptical roundest and intermediate virions. As shown in figure 6.9, the GP, Z and NP regions of the virion show a periodicity with high protein content indicated by high electron density at the ends (0^0 and 180^0) lower protein content at the sides (90^0 and 270^0) and intermediate protein content in between (45^0, 135^0, 225^0 and 315^0).

This effect was greatest on elliptical particles, intermediate on intermediate particles and least on round particles, which displayed uniform protein density.

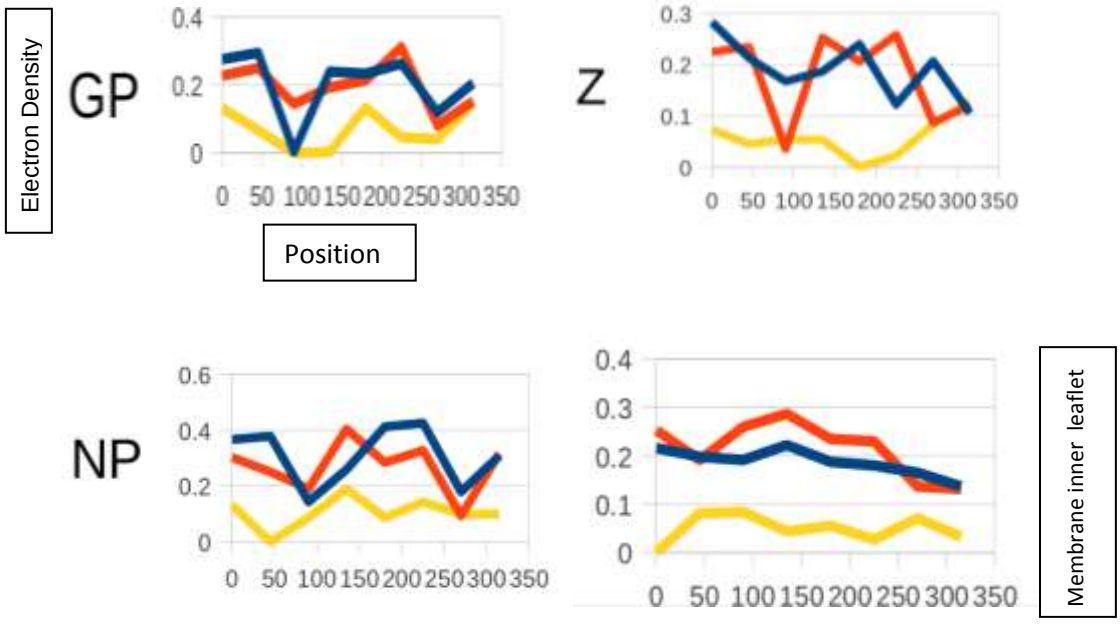

Figure 6:9. (A) Blue line represent the most elliptical viruses (B) Red line represents the intermediate virus particle means neither elliptical nor round ones (C) Yellow line represents the roundest virus particles.

6.9 NP Density:

To better assess the architectural differences in round and elliptical particles, density in the region where NP was expected (IT-2 in Neuman *et al* [120]) was plotted against shape for groups of particles. Each group contained 5% of the available particle data, sorted according to virion shape. From this data it was concluded that low NP density in IT-2 near the inner leaflet of the virion membrane was associated with elliptical morphology. This may give a clue to the mechanism by which elliptical particles arise either from miss-assembly (marked by low NP density in IT-2) or from local disruption of the GP-Z-NP complexes (figure 6.10).

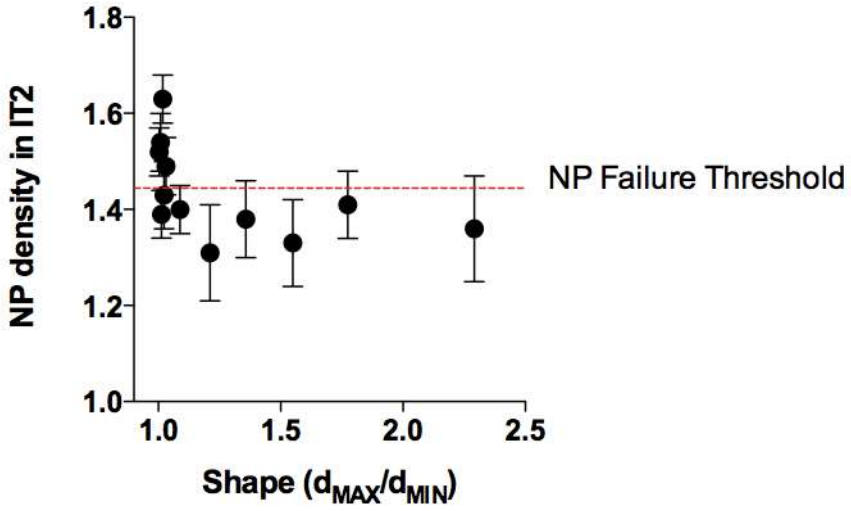

Figure 6:10. This figure shows NP density versus shape.

6.10 Comparison of inner to outer leaflet and outer leaflet density:

In order to understand the density of vesicles as compare to the arenaviruses, and the ratio of various vesicles was taken and plotted the transect plots. Here we are trying to make an assay to detect that how much protein is inserted in the membrane so I have looked at the vesicles from lots of different sources and groups. It was concluded that ratio of inner to outer is constant in vesicles (see figure 6:11).

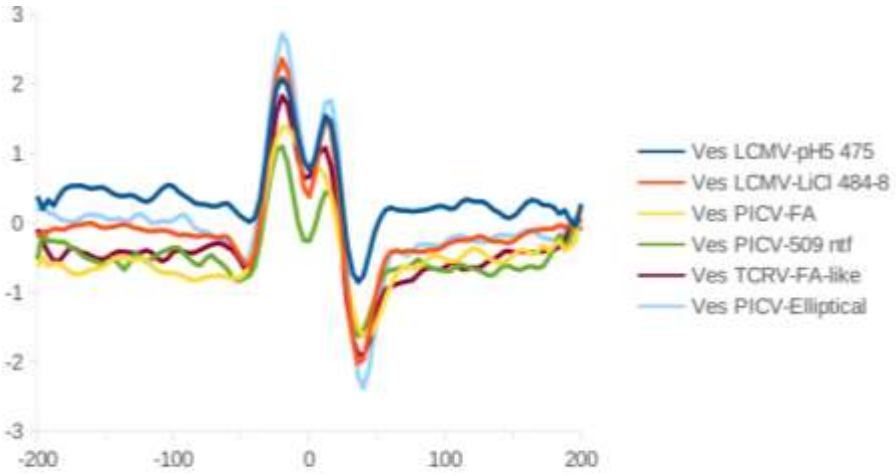

Figure 6.11 Ratio of inner to outer leaflet density is constant for vesicles.

6.11 Comparison of PICV native and fusion activated with the vesicles:

In order to understand the inner to outer and outer leaflet density the data of vesicles from various sources and groups and PICV native and fusion activated was calculated from transect plot. It was concluded that the ratio of outer leaflet density is constant where inner to outer leaflet density is variable (figure 6.11 and 6.12). The most proteins are in the inner leaflet of native PICV and the least in vesicles as evidenced by increasing electron density of the inner leaflet relative to the outer leaflet membrane (figure 6.13).

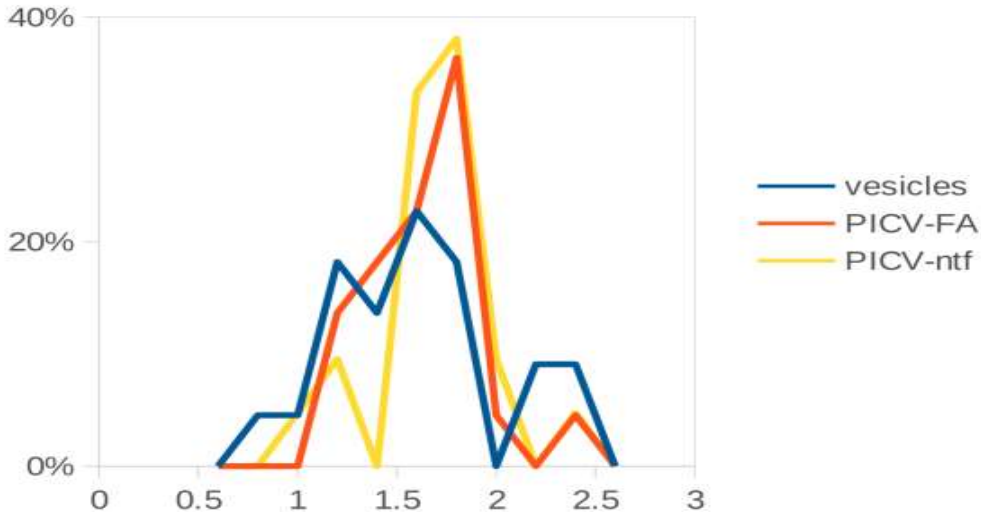

Figure 6:12. Outer leaflet density is constant in PICV.

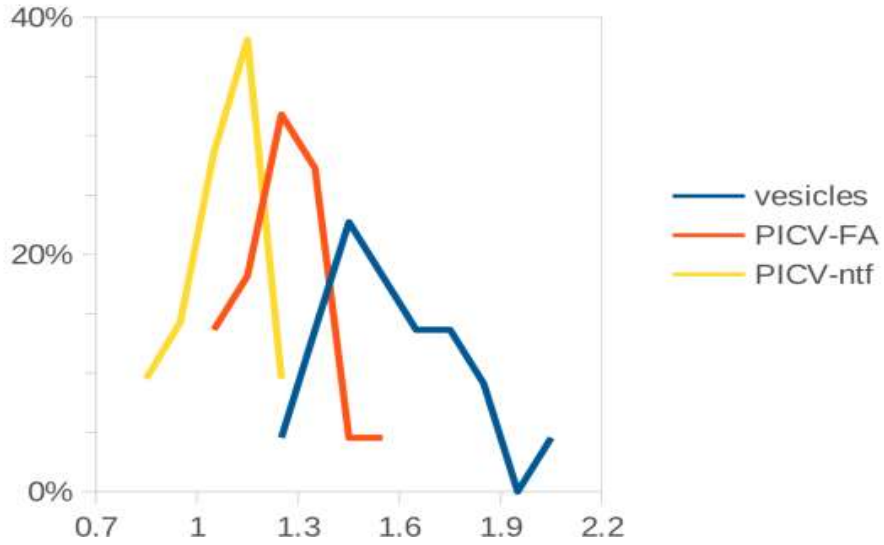

Figure 6:13. Ratio of inner to outer leaflet is variable in PICV and vesicles from different sources and groups.

6.12 Comparison of LCMV native and fusion activated with the vesicles:

In order to understand the relative density of the membrane leaflets of LCMV and TCRV the analysis was repeated. As for PICV, LCMV particles showed an increasing protein content of the inner leaflet compared to co-purified vesicles membranes from the same micrograph (figure 6.14), while outer leaflet density was similar (figure 6.15).

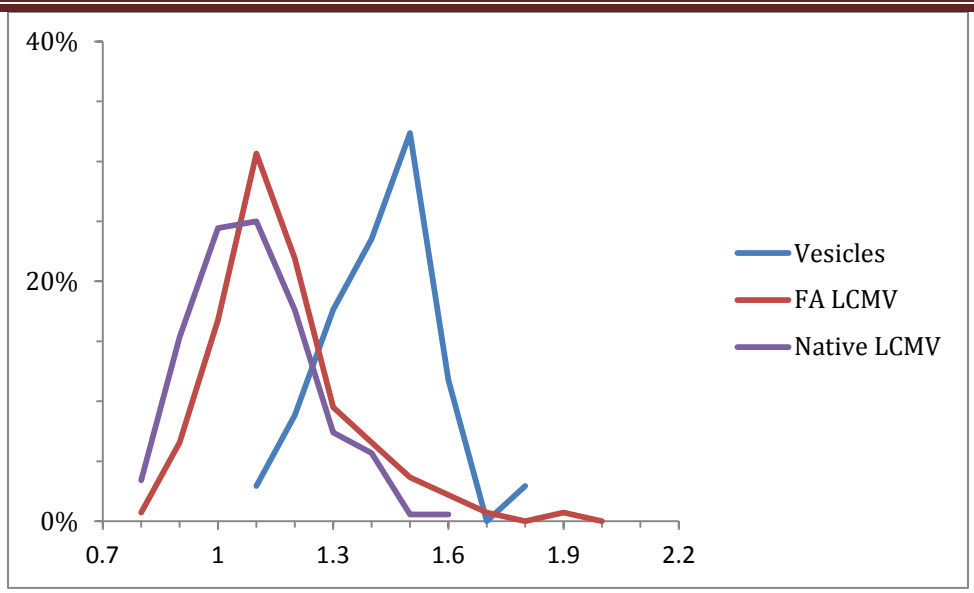

Figure 6:14. Ratio of outer to inner leaflet density.

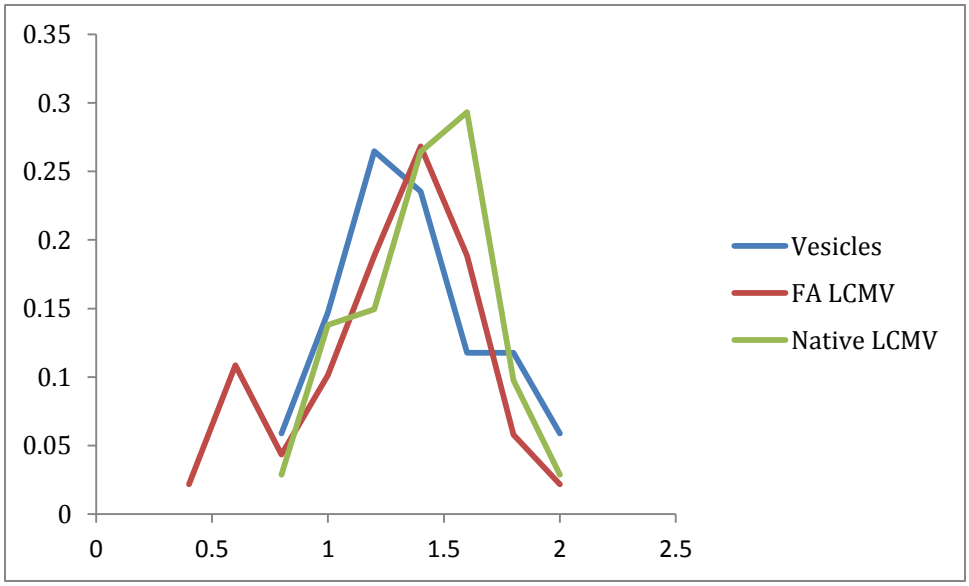

Figure 6:15. Outer leaflet density only in LCMV.

6.13 Comparison of TCRV native and fusion activated with the vesicles:

Similar results were also obtained for TCRV (figure 6.16 and 6.17) suggesting that all arenavirus particles have considerable protein content in the inner bilayer leaflet. A second interesting effect was that fusion activation (PICV and LCMV) produced particles with an intermediate protein density in the inner leaflet, suggesting that some protein had been removed from the inner face of the membrane.

Fusion activated TCRV were not available for analysis, but 20 particle (about 0.5% of the dataset) were identified that had no visible surface GP and had disorganized interior, similar to fusion-activated LCMV and PICV particles. These also showed an immediate inner leaflet protein content as expected (figure 6.16).

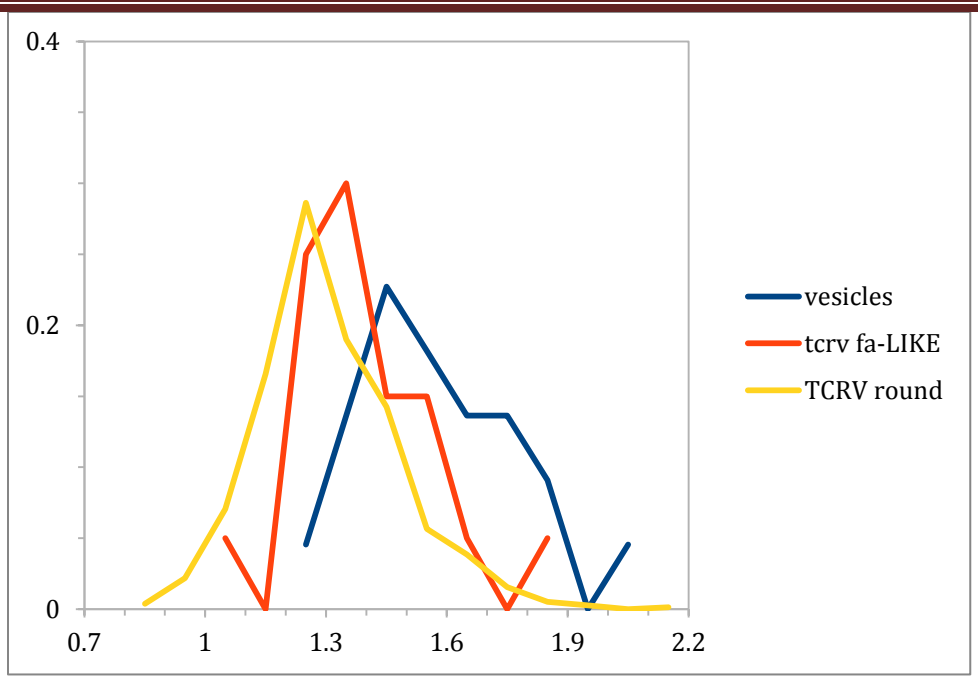

Figure 6.16: Ratio of outer to inner leaflet density in TCRV

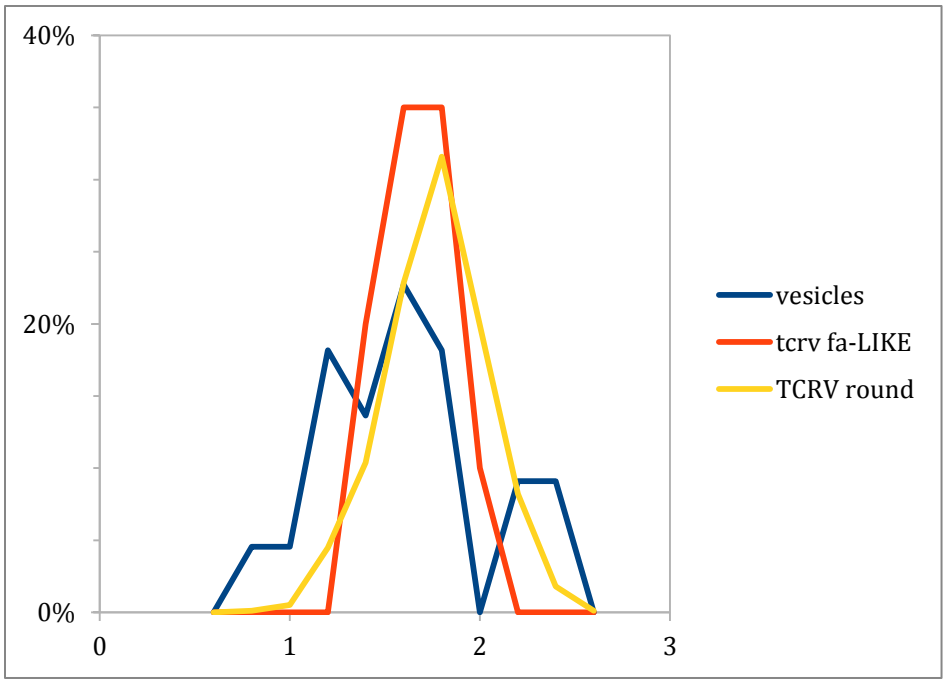

Figure: 6.17. Outer leaflet density only in TCRV

6.14 Discussion.

From this chapter it it was discovered that arenavirus shape is controlled by complexes containing GPC, Z and NP at the surface of the virion, and that an unbroken inner shell of NP is essential for maintaining a rigid spherical shape. Furthermore, it was revealed that the inner leaflet of intact arenaviruses has a lower density than the inner leaflet of vesicles consistent with the interpretation that viral proteins are displaying lipid molecules from the inner leaflet of the viral membrane.

Conclusions

The result of density transects analysis of the ends (0^0 and 180^0) vs sides (90^0 and 270^0) of elliptical TCRV are shown in figure 6.7. While the density of the inner and outer membrane peaks remained constant, there was less electron density present in the expected positions of GP, Z and NP on the flat "sides" (90^0 and 270^0) of elliptical TCRV particles. The shape of each peak was similar, but no broadening was observed.

References

1. Salvato, M., Clegg JCS,Buchmeier MJ,Charrel RN, Gonzales JP,Lukashevish IS, Peters CJ, Rico-Hesse R, Romanoswski V, ed. *Family Arenaviridae*. ed. B.L. Van Regenmortel MHV. Vol. Eigth. 2005: Los Angless. 725-738.
2. Charrel, R.N. and X. de Lamballerie, *Zoonotic aspects of arenavirus infections.* Vet Microbiol, 2009.
3. Childs JE, P.C., *Ecology and Epidemiology of arenavirus and their hosts*, in *The Arenavirus*, M.S. Salvato, Editor. 1993, plenum Press: New York. p. 331-384.
4. Riviere, Y., et al., *The S RNA segment of lymphocytic choriomeningitis virus codes for the nucleoprotein and glycoproteins 1 and 2.* J Virol, 1985. **53**(3): p. 966-8.
5. Auperin, D.D., et al., *Sequencing studies of pichinde arenavirus S RNA indicate a novel coding strategy, an ambisense viral S RNA.* J Virol, 1984. **52**(3): p. 897-904.
6. Auperin, D.D., D.R. Sasso, and J.B. McCormick, *Nucleotide sequence of the glycoprotein gene and intergenic region of the Lassa virus S genome RNA.* Virology, 1986. **154**(1): p. 155-67.
7. Wilson, S.M. and J.C. Clegg, *Sequence analysis of the S RNA of the African arenavirus Mopeia: an unusual secondary structure feature in the intergenic region.* Virology, 1991. **180**(2): p. 543-52.
8. Romanowski, V. and D.H. Bishop, *Conserved sequences and coding of two strains of lymphocytic choriomeningitis virus (WE and ARM) and Pichinde arenavirus.* Virus Res, 1985. **2**(1): p. 35-51.
9. Salvato, M., E. Shimomaye, and M.B. Oldstone, *The primary structure of the lymphocytic choriomeningitis virus L gene encodes a putative RNA polymerase.* Virology, 1989. **169**(2): p. 377-84.
10. Conzelmann, K.K., *Genetic manipulation of non-segmented negative-strand RNA viruses.* J Gen Virol, 1996. **77 (Pt 3)**: p. 381-9.
11. Auperin, D.D. and J.B. McCormick, *Nucleotide sequence of the Lassa virus (Josiah strain) S genome RNA and amino acid sequence comparison of the N and GPC proteins to other arenaviruses.* Virology, 1989. **168**(2): p. 421-5.
12. Salvato, M.S. and E.M. Shimomaye, *The completed sequence of lymphocytic choriomeningitis virus reveals a unique RNA structure and a gene for a zinc finger protein.* Virology, 1989. **173**(1): p. 1-10.
13. Francis, S.J. and P.J. Southern, *Molecular analysis of viral RNAs in mice persistently infected with lymphocytic choriomeningitis virus.* J Virol, 1988. **62**(4): p. 1251-7.
14. Iapalucci, S., N. Lopez, and M.T. Franze-Fernandez, *The 3' end termini of the Tacaribe arenavirus subgenomic RNAs.* Virology, 1991. **182**(1): p. 269-78.
15. Southern, P.J., et al., *Molecular characterization of the genomic S RNA segment from lymphocytic choriomeningitis virus.* Virology, 1987. **157**(1): p. 145-55.
16. Fuller-Pace, F.V. and P.J. Southern, *Detection of virus-specific RNA-dependent RNA polymerase activity in extracts from cells infected with lymphocytic choriomeningitis virus: in vitro synthesis of full-length viral RNA species.* J Virol, 1989. **63**(5): p. 1938-44.
17. Fuller-Pace, F.V. and P.J. Southern, *Temporal analysis of transcription and replication during acute infection with lymphocytic choriomeningitis virus.* Virology, 1988. **162**(1): p. 260-3.
18. Buchmeier, M.J., *Arenaviruses: protein structure and function.* Curr Top Microbiol Immunol, 2002. **262**: p. 159-73.
19. Gallaher, W.R., C. DiSimone, and M.J. Buchmeier, *The viral transmembrane superfamily: possible divergence of Arenavirus and Filovirus glycoproteins from a common RNA virus ancestor.* BMC Microbiol, 2001. **1**: p. 1.
20. Eichler, R., et al., *Identification of Lassa virus glycoprotein signal peptide as a trans-acting maturation factor.* EMBO Rep, 2003. **4**(11): p. 1084-8.
21. Eichler, R., et al., *Signal peptide of Lassa virus glycoprotein GP-C exhibits an unusual length.* FEBS Lett, 2003. **538**(1-3): p. 203-6.
22. Froeschke, M., et al., *Long-lived signal peptide of lymphocytic choriomeningitis virus glycoprotein pGP-C.* J Biol Chem, 2003. **278**(43): p. 41914-20.

23. Borden, K.L., E.J. Campbell Dwyer, and M.S. Salvato, *An arenavirus RING (zinc-binding) protein binds the oncoprotein promyelocyte leukemia protein (PML) and relocates PML nuclear bodies to the cytoplasm.* J Virol, 1998. **72**(1): p. 758-66.
24. Borrow, P. and M.B. Oldstone, *Mechanism of lymphocytic choriomeningitis virus entry into cells.* Virology, 1994. **198**(1): p. 1-9.
25. Calain, P. and L. Roux, *The rule of six, a basic feature for efficient replication of Sendai virus defective interfering RNA.* J Virol, 1993. **67**(8): p. 4822-30.
26. Beyer, W.R., et al., *Endoproteolytic processing of the lymphocytic choriomeningitis virus glycoprotein by the subtilase SKI-1/S1P.* J Virol, 2003. **77**(5): p. 2866-72.
27. Pinschewer, D.D., et al., *Recombinant lymphocytic choriomeningitis virus expressing vesicular stomatitis virus glycoprotein.* Proc Natl Acad Sci U S A, 2003. **100**(13): p. 7895-900.
28. York, J., et al., *The signal peptide of the Junin arenavirus envelope glycoprotein is myristoylated and forms an essential subunit of the mature G1-G2 complex.* J Virol, 2004. **78**(19): p. 10783-92.
29. Buchmeier, M.J.B., M.D.,Peters,J.S., *Arenaviridae:The viruses and their replication.* 2001, Philadelphia: Williams and Wilkins. 1635-1668.
30. Cao, W., et al., *Identification of alpha-dystroglycan as a receptor for lymphocytic choriomeningitis virus and Lassa fever virus.* Science, 1998. **282**(5396): p. 2079-81.
31. Kunz, S., P. Borrow, and M.B. Oldstone, *Receptor structure, binding, and cell entry of arenaviruses.* Curr Top Microbiol Immunol, 2002. **262**: p. 111-37.
32. Kunz, S., et al., *Molecular analysis of the interaction of LCMV with its cellular receptor [alpha]-dystroglycan.* J Cell Biol, 2001. **155**(2): p. 301-10.
33. Pinschewer, D.D., M. Perez, and J.C. de la Torre, *Role of the virus nucleoprotein in the regulation of lymphocytic choriomeningitis virus transcription and RNA replication.* J Virol, 2003. **77**(6): p. 3882-7.
34. Kunz, S., et al., *Mechanisms for lymphocytic choriomeningitis virus glycoprotein cleavage, transport, and incorporation into virions.* Virology, 2003. **314**(1): p. 168-78.
35. Ilaria, R.L., Jr., R.G. Hawley, and R.A. Van Etten, *Dominant negative mutants implicate STAT5 in myeloid cell proliferation and neutrophil differentiation.* Blood, 1999. **93**(12): p.